RESEARCH ARTICLE

CrossMark

Patterns and controls of mercury accumulation in sediments from three thermokarst lakes on the Arctic Coastal Plain of Alaska

S. M. Burke[1] · C. E. Zimmerman[2] · B. A. Branfireun[3] · J. C. Koch[2] · H. K. Swanson[1]

Abstract

The biogeochemical cycle of mercury will be influenced by climate change, particularly at higher latitudes. Investigations of historical mercury accumulation in lake sediments inform future predictions as to how climate change might affect mercury biogeochemistry; however, in regions with a paucity of data, such as the thermokarst-rich Arctic Coastal Plain of Alaska (ACP), the trajectory of mercury accumulation in lake sediments is particularly uncertain. Sediment cores from three thermokarst lakes on the ACP were analyzed to understand changes in, and drivers of, Hg accumulation over the past ~100 years. Mercury accumulation in two of the three lakes was variable and high over the past century (91.96 and 78.6 µg/m²/year), and largely controlled by sedimentation rate. Mercury accumulation in the third lake was lower (14.2 µg/m²/year), more temporally uniform, and was more strongly related to sediment Hg concentration than sedimentation rate. Sediment mercury concentrations were quantitatively related to measures of sediment composition and VRS-inferred chlorophyll *a*, and sedimentation rates were related to various catchment characteristics. These results were compared to data from 37 previously studied Arctic and Alaskan lakes. Results from the meta-analysis indicate that thermokarst lakes have significantly higher and more variable Hg accumulation rates than non-thermokarst lakes, suggesting that certain properties (e.g., thermal erosion, thaw slumping, low hydraulic conductivity) likely make lakes prone to high and variable Hg accumulation rates. Differences and high variability in Hg accumulation among high latitude lakes highlight the complexity of predicting future climate-related change impacts on mercury cycling in these environments.

Keywords Mercury · Thermokarst · Paleolimnology · Alaska · Lake · Sediment

✉ H. K. Swanson
heidi.swanson@uwaterloo.ca

S. M. Burke
samantha.burke2@gmail.com

1 Department of Biology, University of Waterloo, Waterloo, ON, Canada

2 US Geological Survey, Alaska Science Center, Anchorage, AK, USA

3 Department of Biology and Centre for Environment and Sustainability, University of Western Ontario, London, Canada

Introduction

Mercury (Hg), in an organic, methylated form (monomethylmercury; MeHg), is a neurotoxicant that bioaccumulates and biomagnifies through aquatic food webs (see Kidd et al. 1995; Atwell et al. 1998; Lockhart et al. 2005), and can reach concentrations in fish that are harmful to fish-eating wildlife and humans. Post-industrial (ca.1850) increases in Hg emitted to the atmosphere can largely be attributed to the combustion of coal (Driscoll et al. 2013). In North America, Hg emissions from the power sector have decreased from their peak in the 1980s due to emissions controls (Slemr et al. 2003); however, there have been recent increases in coal combustion (and thus, Hg emissions) for electricity production in other regions, including Asia. In addition, other industrial activities, such as artisanal gold mining, are emerging as significant contributors to the global atmospheric pool of Hg (see UNEP, 2013), thus making the future of Hg emissions unclear. Changes in Hg deposition, and the

degree to which anthropogenic emissions have contributed to the pool of Hg in aquatic ecosystems, are often assessed using paleolimnological approaches, as lake sediments can act as a natural archive in the absence of an instrumental record.

In combination with sedimentation rates, mercury concentrations in dated lake sediment cores are used to produce reliable records of historical Hg accumulation rates (e.g., Biester et al. 2007). Numerous studies have reconstructed historical Hg accumulation rates in lake sediments (e.g., Yang and Rose 2003; Fitzgerald et al. 2005; Drevnick et al. 2012), and found near ubiquitous increases in Hg accumulation rates from pre-industry (pre ca. 1850) to present. Ratios of modern to pre-industry Hg concentrations (termed enrichment factors), or Hg accumulation rates (termed flux ratios), are often used to assess anthropogenically driven changes in lake sediment Hg (e.g., Landers et al. 1998; Bindler et al. 2001). Studies conducted at temperate latitudes have reported a large range of Hg flux ratios in lake sediments; 2.1–6.9 in Vermont and New Hampshire (Kamman and Engstrom 2002), 3.6–9.8 in Minnesota (Engstrom et al. 2007), and 1.6–5.7 (Lorey and Driscoll 1999) and 3–30 (Bookman et al. 2008) in New York. Variability in flux ratios among these temperate lakes can largely be explained by distance from point sources of Hg emissions.

Results from studies conducted on sediment cores from Arctic lakes indicate that increases in Hg flux have occurred from ~ 1850 to modern times, and that these increases are in general more modest (a mean flux ratio of 3) than many of those observed in temperate systems (see Landers et al. 1998)—reflecting greater distance from point sources. Increases in Hg flux from pre-industry to modern times (a flux ratio > 1) have been described for 53 of 56 Arctic lakes reported in eight different primary and synthesis publications (Hermanson 1998; Landers et al. 1998; Bindler et al. 2001; Outridge et al. 2007; Muir et al. 2009; Drevnick et al. 2012, 2016; Deison et al. 2012). Reported modern Hg fluxes for lakes in the aforementioned studies varied by ~ 30-fold (mean of 14 $\mu g/m^2$/year), while Hg concentrations for these same lakes varied ~ threefold (mean of 150 ng/g).

Although increases in the global atmospheric pool of Hg since pre-industry have resulted in increases in Hg accumulation in the vast majority of lakes studied, the degree of increase varies, and some of this variation is due to among-lake differences in physical and biological characteristics of lakes and catchments. Relative catchment size affects the rate at which atmospherically derived Hg is delivered to both Arctic (see Drevnick et al. 2012) and temperate (Grigal et al. 2002) lakes. Lakes that have greater catchment to lake area ratios (relative catchment sizes) have been found to respond to changes in atmospheric Hg emissions more slowly than those with smaller catchment to surface area ratios, due to the storage and gradual release of "legacy" Hg in catchment

vegetation, litter, soil and groundwater (see Grigal 2002; Harris et al. 2007). Catchment soil composition also affects delivery of Hg to lakes and lake sediments. Mercury (either anthropogenic or natural) that is retained in catchment soils is often strongly sorbed to organic matter (OM), and thus the amount of OM and the rate of OM decomposition can affect the magnitude and timing of release of Hg from catchments to downstream lakes (see Grigal 2002). In thermokarst lakes that receive drainage from OM-rich peats, Hg delivery to lakes can also be affected by degradation of permafrost.

The potential contribution of legacy Hg (stored in the catchment) to lake sediments is particularly large for Arctic thermokarst lakes. 'Thermokarst' refers to the process by which ice-rich permafrost soils degrade, causing land subsidence, water impoundment, and the formation and expansion of surface water bodies, such as lakes. Over 20% ($3.6 \times 10^6 km^2$) of the northern permafrost region is characterized as thermokarst landscape (Olefeldt et al. 2016). Recently, Olefeldt et al. (2016) delineated the areal extent of three different categories of thermokarst landscape—hillslope, lake, and wetland—using a conceptual modeling framework that accounted for presence of distinct thermokarst landforms and other landscape characteristics, such as ground ice content, terrestrial ecoregion, and presences of permafrost peat soils (histels). 'Lake thermokarst' landscapes are characterized by lake initiation, expansion, drainage, and drainage basin formation (Olefeldt et al. 2016). 'Wetland thermokarst' landscapes are characterized by landforms such as thermokarst bogs, fens, and shore fens, and 'hillslope thermokarst' landscapes by active layer detachment slides, retrogressive thaw slumps, thermal erosion gullies, beaded streams, and thermokarst water tracks (Olefeldt et al. 2016).

Rising temperatures resulting from climate change affect the frequency and magnitude of thermokarstic processes (e.g., thermal erosion, catastrophic drainages, and retrogressive thaw slumps; see Grosse et al. 2013), and thus Hg delivery to lakes. Thermokarst lakes are formed through degradation of ground ice, and once a thermokarst lake is formed, it tends to grow laterally through thermal and mechanical erosion into adjacent ice-rich permafrost deposits and soils, which can lead to shoreline collapse (Jorgenson and Shur 2007; see; Grosse et al. 2013). When a lake expands via thermal erosion, large amounts of soil or sediment, which contain bound Hg, are mobilized and deposited into the lake (see Grosse et al. 2013). The amount of Hg deposited is largely dependent on soil and sediment characteristics, and the degree of interaction with atmospherically-deposited Hg over time (Oswald et al. 2014). Thermokarstic events that affect catchments with soils rich in organic matter (OM) may result in relatively high Hg delivery to lakes, as soil OM generally has higher Total Hg (Oswald et al. 2014) and a greater proportion as MeHg (see Bravo et al. 2017), whereas

thermokarstic events that affect catchments with soils rich in minerogenic matter could result in Hg concentrations being diluted in lake sediments (Deison et al. 2012).

Rising temperatures can also influence the delivery of Hg to lake sediments by increasing lake primary production (Outridge et al. 2007). In previous studies, a large portion of post-industrial increases in Hg in Arctic lake sediments has been attributed to increases in autochthonous primary production and algal scavenging (Outridge et al. 2007; Stern et al. 2009). The 'algal-scavenging hypothesis' originated from observed positive relationships between sediment Hg concentration and S2 carbon (the algal-derived component of organic carbon). Kirk et al. (2011) found, however, that in 7 of 14 Arctic lakes, the relationship between sediment Hg concentration and algal S2 carbon content was not significant, suggesting that changes in sediment Hg concentrations and fluxes could not be attributed to changes in primary production alone.

The Arctic Coastal Plain of Alaska is a 'lake thermokarst' region that stretches from the Brooks Range (68°N) to the Arctic Ocean (71°N), and covers an area of approximately 300,000 km^2. There is a paucity of information (i.e., no down-core studies) on Hg accumulation in sediments for lakes on the Arctic Coastal Plain compared to other regions in Alaska and the Arctic. Studies of temporal patterns in Hg accumulation have been completed on higher relief lakes further south in Alaska that are not formed or affected by thermokarst processes (e.g., Allen-Gil et al. 1997; Engstrom and Swain 1997; Landers et al. 1998; Fitzgerald et al. 2005). Fitzgerald et al. (2005) found that Hg accumulation rates in foothills lakes near the Brooks Range (64°N, 147°W) had increased three-fold since ca. 1850, indicating anthropogenically driven increases in Hg delivery to these lakes. Based on the finding that pre-industrial Hg accumulation rates in sediment were higher than those found in other Arctic lakes, Fitzgerald et al. (2005) also concluded that erosional inputs of Hg to lakes in the Brooks Range were relatively more important than in other Arctic lakes. Concentrations of Hg and other metals have been found to be naturally elevated in sediments of Arctic Alaskan lakes relative to uncontaminated lakes in other Arctic and temperate regions, due to mineral rich soils (Allen-Gil et al. 1997). The importance of erosional inputs of naturally derived Hg to thermokarst lakes on the Arctic Coastal Plain is unknown.

Our overall objective was to consider dominant controls on, and variability among, sediment Hg accumulation rates in Arctic and subarctic lakes. Specifically, we aimed to: (1) characterize patterns of Hg accumulation over the past ~100 years in sediments of three Arctic Coastal Plain lakes in Alaska; (2) identify factors (e.g. chl a concentration, organic matter content, sedimentation rate) that influenced patterns of sediment Hg accumulation, and compare results among the three study lakes; and, (3) collate mercury accumulation and other sediment proxy data from previously-published studies on Arctic and sub-Arctic lakes ($n = 37$), and interpret sediment Hg accumulation rates in the context of thermokarst landscape types. Results were interpreted in the context of evaluating how changing climate could affect Hg accumulation rates in Arctic thermokarst lakes.

Materials and methods

Study area

The three lakes for which primary data were collected for this study are located on the Arctic Coastal Plain of Alaska, an area that extends north from the foothills of the Brooks Range (68°N) to the Chukchi and Beaufort Seas (71°N). The lakes are located on low-relief tussock Tundra within a zone of continuous permafrost, and span a distance of three degrees of latitude. Selected from a larger set of lakes monitored by the Circum-Arctic Lakes Observation Network (http://arcticlakes.org), the lakes are (north to south) Barrow 100 (BRW100), Atqasuk 206 (ATQ206), and Reindeer Camp 312 (RDC312; Fig. 1). These lakes are representative of other thermokarst lakes in the northern permafrost region, as they occupy depressions formed by the degradation of ground ice and rely on snowmelt and summer rainfall to maintain a water balance (Grosse et al. 2013). Specific location and physiographic information about the study lakes is in Table 1.

Sample collection and preparation

In August 2014, sediment cores were collected in duplicate (to provide sufficient mass for future analyses) from each of the three lakes, using a Glew gravity corer fitted with 10 cm diameter Lexan® tubes. Sediments were extruded into 0.5 cm segments with a Glew extruder, placed in 4 oz Whirlpak® bags, and kept in the dark at 4 °C while in transit to the laboratory at the University of Waterloo (Waterloo, Ontario, Canada). Samples were then stored in the dark at 4 °C before ~0.5 g subsamples of each core segment were analyzed for loss on ignition (LOI) to quantify percent organic matter (%OM) and percent mineral matter (%MM). LOI analyses were completed at the WATER lab at the University of Waterloo, following methods from Dean (1974).

Sediment dating and sedimentation rates

Freeze-dried subsamples of sediment from 1 cm intervals were analyzed from one core from each lake to determine total and supported ^{210}Pb activity using an Ortec co-axial HPGe Digital Gamma Ray (Ortec GWL-120-15)
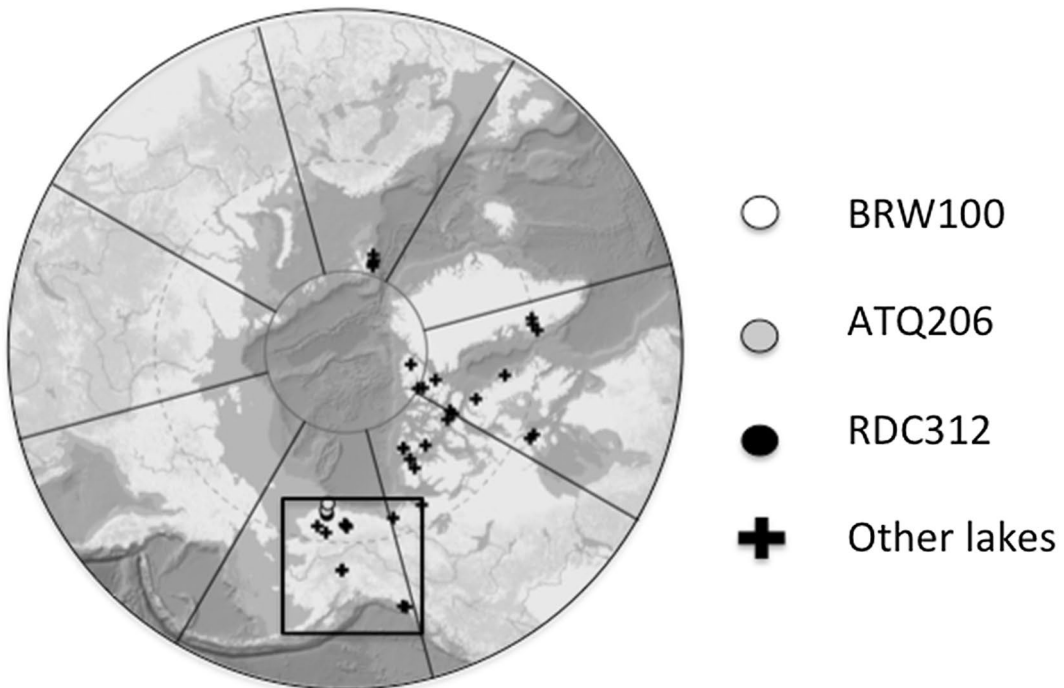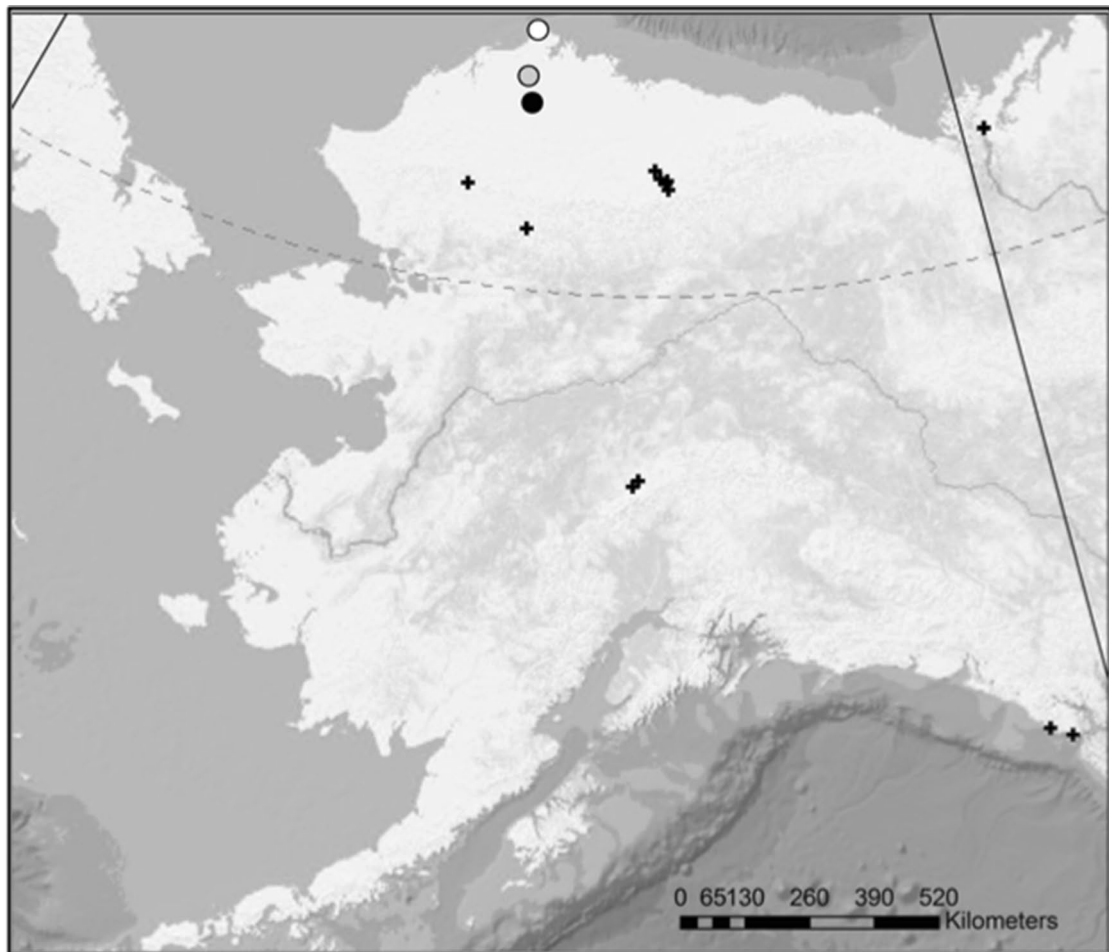
Fig. 1 Study lakes on the Arctic Coastal Plain of Alaska (BRW 100, ATQ 206, RDC 312) and other lakes with published sediment Hg accumulation data; circles represent lakes in this study, crosses represent comparison lakes

Table 1 Physical characteristics and summary Hg accumulation results of the three study lakes (BRW100, ATQ206, RDC312) on the Arctic Coastal Plain of Alaska; Hg accumulation trends were assessed using Mann–Kendall tests (a p value < 0.05 denotes a significant temporal trend and the Kendall's tau denotes the direction and magnitude of the relationship); McLeod (2011); catchments were delineated, and percent growth was calculated using ArcMap™10.2.2 (ESRI 2016)

	BRW100	ATQ206	RDC312
Latitude (decimal degrees)	71.24163	70.41557	69.95348
Longitude (decimal degrees)	− 156.77391	− 156.98128	− 156.63817
Surface area (km^2)	17.6	16.8	6.6
Catchment area (km^2)	236.6	209.9	265.2
Catchment to surface area ratio	13.4	12.5	40.4
Growth since 1948 (%)	12.7	− 0.3	5.4
Landscape type	Lake thermokarst	Lake thermokarst	Lake thermokarst
Mean Hg accumulation (µg/m^2/year)	92.0	14.2	78.7
Standard deviation	36.1	3.6	68.5
Hg accumulation trend	No trend	Positive	No trend
Kendall's tau (τ)	0.28	0.42	0.61
Mann–Kendall p value	0.17	0.04	0.84

Spectrometer interfaced with Maestro 32 software (version 5.32; Ortec, 2006) at the University of Waterloo's WATER Lab.

Chronologies for each sediment core were developed using the constant rate of supply model (Appleby and Oldfield 1978), which assumes that the flux of ^{210}Pb from the atmosphere is constant and adjusts for variations in sedimentation rate. Sedimentation rates were calculated using ^{210}Pb dates and cumulative dry mass. All subsequent analyses were completed on sediment from the one core in each lake for which chronologies were developed.

Total mercury analysis

Total mercury analysis was completed on homogenized freeze-dried sediment at 1 cm intervals (beginning at 0.5 cm) at the Biotron Centre for Experimental Climate Change Research at Western University (London, Ontario, Canada). Sample sizes were approximately 50 mg. Analyses were completed on a Milestone® DMA-80 Direct Mercury Analyzer in accordance with U.S. EPA method 7473 (U.S. EPA, 2007). A certified reference material (MESS-3; Marine Sediment Certified Reference Materials from the National Research Council, Ottawa, Ontario) was analyzed at the start of each run and after every 10 samples (mean recovery: 109.9% ± 15.3 SD, $n = 9$). Blanks were analyzed at the start of each run and after every 10 samples ($n = 4$). All Hg concentrations are expressed as ng/g dry weight.

VRS-inferred chlorophyll *a* analysis

Chlorophyll *a* (Chl *a*) concentrations were inferred using visual reflectance spectroscopy (VRS) at the Paleoecological Environmental Assessment and Research Lab (PEARL) at Queen's University (Kingston, Ontario, Canada). The VRS method provides a means to infer changes in whole lake primary production, as it detects chlorophyll *a* and

its derivatives, which negates the need to account for pigment diagenesis (Michelutti et al. 2010). Briefly, sediments (from intervals alternate to those used for Hg analyses) were freeze-dried and sieved to 125 µm to homogenize the samples and improve replication. Following this, sediment from each interval was analyzed using a FOSS NIRS (Near Infrared Spectrophotometer) system Model 6500 rapid content analyzer to obtain sediment reflectance. For each interval, chlorophyll *a* concentrations were inferred based on the measured amplitude of a trough in percent reflectance at 650–700 nm wavelengths (the red portion of the spectrum; Wolfe et al. 2006).

Aerial imagery analysis

Historical aerial imagery was obtained from the United States Geological Survey EarthExplorer https://earthexplorer.usgs.gov/ (USGS 2016). These images were geo-referenced using the ArcGIS™World Imagery Basemap (ESRI 2016). The geo-referenced lakes were manually converted into polygons, and surface areas were calculated to quantify changes in lake surface area over time. Surface area of Arctic Coastal Plain lakes tends to increase in spring and early summer due to snow melt. We therefore chose to quantify and compare lake surface areas between 1948 and 2005, as images in these years were captured on Aug 2nd and Aug 1st, respectively. Obvious physical changes within the catchment were also noted using all images. All aerial imagery analyses were completed using ArcMap™10.2.2 (ESRI 2016).

Comparisons with other Arctic and subarctic lakes

To provide further context for results, and to compare Hg accumulation rates from our study to other studies, a literature search for available published down-core data from other Alaskan and Arctic lakes was conducted. Overall,

data were compiled for 37 additional lakes (33 Arctic, 4 Alaskan subarctic; Fig. 1; Table 2; see Online Resource 1). If accumulation rates were not reported, sedimentation rate and mercury concentration were used to calculate them. Where raw or tabular data were not available, values were extracted from published figures using WebPlotDigitizer v3.10 (Rohatgi 2016). To account for in-lake matter transfer and to strengthen among-lake comparisons, focus-corrected accumulation rates were used when focusing factors

were available. Uncorrected rates were used when focusing factors were not available. All lakes, including the three lakes sampled, were assigned a landscape type (hillslope thermokarst, lake thermokarst, non-thermokarst) based on their coordinates and the maps generated by Olefeldt et al. (2016); a lake was assigned a designation if the dominant landscape type had moderate (10–30%) or high (30–60%) coverage of a particular landscape type. All data and metadata are located in the Online Resource 1.

Table 2 Mean Hg accumulation and Mann–Kendall results for thirty-seven previously studied Arctic and subarctic lakes; landscape types were designated using the maps generated by Olefeldt et al. 2016; further lake information available in the Supplemental Materials

Lake	Country	Landscape type	Mean Hg Accum ($\mu g/m^2$/year)	σ	Trend	τ	p
2-A	Canada	Lake	62.23	18.04	neg	− 0.71	0.019
2-B	Canada	Lake	23.88	13.58	pos	0.91	0.007
Amituk	Canada	Non-thermokarst	17.98	7.48	pos	0.70	0.02
AX-AJ	Canada	Hillslope	9.85	4.17	pos	0.94	< 0.001
BI-02	Canada	Hillslope	4.94	1.40	pos	0.39	0.047
BK-AH	Canada	Hillslope	4.54	0.98	n/a	− 0.39	0.062
Brady	USA	Non-thermokarst	8.36	1.62	pos	0.46	0.033
Burial	USA	Hillslope	4.40	1.12	pos	0.71	0.019
CF-11	Canada	Non-thermokarst	2.56	1.47	pos	1.00	0.009
Char	Canada	Non-thermokarst	14.38	6.04	pos	0.89	0.0001
Daglet	USA	Non-thermokarst	8.29	1.61	pos	0.78	0.002
Daltjørna	Norway	Non-thermokarst	22.70	4.81	pos	0.78	0.0001
DV-E	Canada	Hillslope	0.89	0.15	n/a	0.67	0.308
Efficient	USA	Hillslope	8.71	3.26	pos	0.64	< 0.0001
Forgetful	USA	Hillslope	10.13	2.66	pos	0.49	0.013
Hazen	Canada	Hillslope	31.55	3.30	n/a	− 0.10	0.442
Lake 53	Greenland	Non-thermokarst	3.69	1.32	pos	0.86	< 0.0001
Lake 70	Greenland	Non-thermokarst	6.23	3.00	n/a	0.41	0.127
Matacharak	USA	Non-thermokarst	3.64	1.52	pos	0.83	0.002
MB-AC	Canada	Hillslope	6.15	1.25	pos	0.84	< 0.0001
MB-S	Canada	Hillslope	2.44	0.14	n/a	0.00	1
Mcleod	USA	Hillslope	17.93	4.73	pos	0.48	0.006
North	Canada	Hillslope	53.96	20.98	pos	0.82	0.0003
Nunatak	Greenland	Non-thermokarst	8.24	1.62	pos	0.81	0.016
Ossian Sarsfjellet	Norway	Non-thermokarst	4.00	1.86	pos	0.72	0.009
Perfect	USA	Hillslope	7.07	1.94	pos	0.88	< 0.0001
Relaxing	USA	Hillslope	2.43	0.97	pos	0.85	< 0.0001
Rocky Basin	Canada	Non-thermokarst	1.26	0.53	pos	1.00	0.03
Romulus	Canada	Hillslope	198.19	67.70	pos	0.78	0.002
Rummy	Canada	Hillslope	13.19	1.83	n/a	0.62	0.072
SHI-L4	Canada	Non-thermokarst	20.00	9.39	pos	0.82	< 0.0001
SHI-L7	Canada	Non-thermokarst	2.64	0.73	n/a	0.17	0.602
Surprise	USA	Hillslope	20.98	11.47	pos	0.90	< 0.0001
Vassauga	Norway	Non-thermokarst	7.30	3.35	pos	0.93	0.002
West	Canada	hillslope	23.44	11.79	pos	0.76	0.006
Wonder	USA	hillslope	31.50	15.31	pos	0.93	0.002
Yterjørna	Norway	non-thermokarst	12.21	9.69	pos	0.84	< 0.0001

Data analysis

Statistical tests were completed using R Studio v 1.0.136 with the core packages in addition to 'Kendall' (McLeod 2011). Figures were generated using either SigmaPlot v11.0 (Systat, 2008) or ArcMap™10.2.2 (ESRI 2016). To determine if there were significant temporal monotonic trends in Hg accumulation, Hg concentration, and chlorophyll *a*, Mann–Kendall tests were completed for the entire core of each of the three study lakes. Mann–Kendall tests were also completed on Hg accumulation rates for each of the 37 lakes for which data were compiled from the literature. Mercury accumulation rates were calculated as the product of sedimentation rate and Hg concentration. To determine which variable accounted for more of the variability in Hg accumulation rate, Hg accumulation rates were related to each of sedimentation rate and Hg concentration using simple linear regressions. To determine if chlorophyll *a* concentrations and/or %OM explained variability in Hg concentrations, sediment Hg concentrations from each lake were related to VRS-inferred chlorophyll *a* concentrations and %OM using simple linear regressions. Finally, to assess how Hg accumulation rates varied among thermokarst landscape types, mean Hg accumulation rates for all 40 lakes (3 sampled in this study, 37 from literature) were compared among lake thermokarst, hillslope thermokarst, and non-thermokarst, landscapes (determined from Olefeldt et al. 2016) with an ANOVA and post-hoc Tukey's test.

Results

Historical changes in lake sediment mercury and primary production

The sediment core used in this study from BRW100, the northernmost study lake, was 16 cm long. The bottom of the core was dated to 1942, suggesting a relatively high rate of sediment accumulation (mean 0.10 ± 0.06 g/cm^2/year). Mercury concentrations ([Hg]) in the BRW 100 core decreased from 101 ng/g to 81 ng/g between 1942 and 2014, and this trend was significant (Fig. 2; Mann–Kendall: S $= -61$, $\tau = -0.58$, p $= 0.002$). A significant increase in VRS-inferred Chl *a* also occurred between 1942 and 2014 (Fig. 2; Mann–Kendall: S $= 117$, $\tau = 0.77$, p $= 0.0001$), suggesting that primary production has increased in BRW 100 since 1942. Mercury accumulation rates were variable (mean $= 91.96 \pm 36.1$ µg/m^2/year), and no significant monotonic trend was detected (Mann–Kendall: S $= -29.0$, $\tau = -0.28$, p $= 0.17$); however, episodic increases in Hg accumulation occurred in ca. 1972, 1983, and 1995, with concomitant increases in sedimentation rate (Fig. 2).
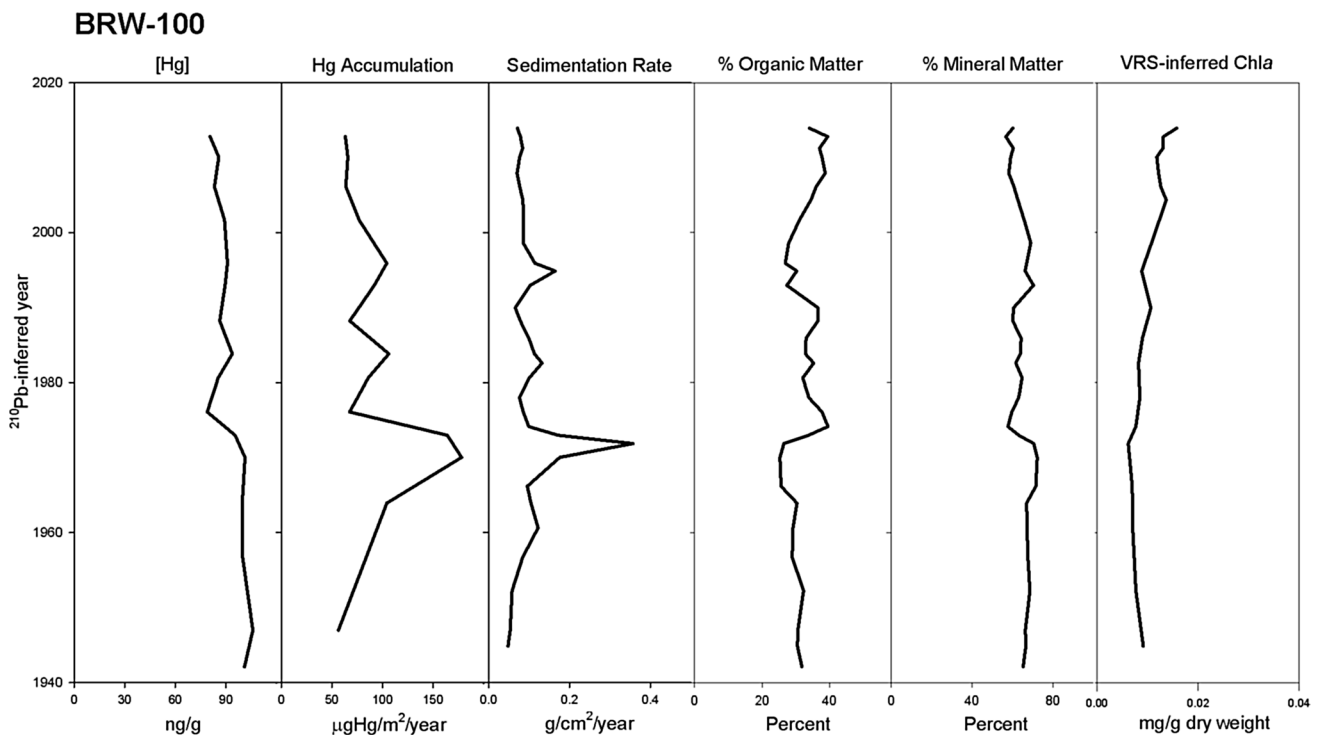

Fig. 2 Temporal profiles of sediment mercury concentration, accumulation rate, sedimentation rate, percent organic matter, percent mineral matter, and VRS-inferred chlorophyll *a* for lake BRW100 on the Arctic Coastal Plain of Alaska sampled in August 2014

The sediment core collected from the latitudinally intermediate lake, ATQ206, was longer than the core from BRW100; the deepest section was 23.5 cm from the surface, and dated to 1878. Sedimentation rate was lower than that observed in BRW100 (mean 0.03 ± 0.01 g/cm^2/year). In contrast to the significant and gradual decrease in sediment [Hg] observed in BRW100, a gradual increase in [Hg] from 28 to 81 ng/g was observed between the early 1880s and the early 1990s, followed by a subsequent decrease to 61 ng/g by 2013; a significant positive trend overall was detected (Fig. 3; Mann–Kendall: $S = 136$, $\tau = -0.648$, $p < 0.001$). Similar to BRW100, a significant increase in VRS-inferred Chl *a* occurred between 1878 and 2014 in ATQ206 (Fig. 2; Mann–Kendall: $S = 125$, $\tau = 0.47$, $p = 0.001$). Mercury accumulation rates (mean 14.2 ± 3.6 µg/m^2/year) increased significantly between the 1880s and 2014, more than doubling from 7.0 to 15 µg/m^2/year (Fig. 3; Mann–Kendall: $S = 107$, $\tau = -0.42$, $p = 0.04$). Although there were overall increases in both [Hg] and Hg accumulation between the top and bottom of the core, sedimentation and accumulation rates inferred from the ATQ206 core were less variable and appreciably lower (sedimentation rates ~ 3–4-fold lower, Hg accumulation rates ~ 5.5–6.5-fold lower) than those from either BRW100 or RDC312 (Figs. 2, 3, 4).

The southernmost lake, RDC312, was dated to 1912 at the bottom of the 12.5 cm core, indicating a sediment accumulation rate (mean 0.13 ± 0.12 g/m^2/year) of similar magnitude to BRW100 and > fourfold higher than ATQ206. Mercury concentration increased significantly between the early 1900s and 2014, from 41 to 60 ng/g (Fig. 4; Mann–Kendall: $S = 46$, $\tau = -0.70$, $p < 0.001$). Unlike the other two lakes, there was not a significant monotonic increase in Chl *a* over time in RDC312 (Mann–Kendall: $S = 38$, $\tau = 0.36$, $p = 0.07$). Mean mercury accumulation rate (78.6 ± 68.5 µg/m^2/year) was more similar to BRW100 (91.96 µg/m^2/year) than to ATQ206 (mean 14.2 µg/m^2/year), and similar to BRW100, Hg accumulation was variable with no significant monotonic trend (Mann–Kendall: $S = 4.0$, $\tau = 0.61$, $p = 0.84$). A periodic increase in Hg accumulation in ca. 1943, along with smaller increases in ca. 1971 and ca. 1986, were coincident with increases in sedimentation rate (Fig. 4). The smaller increases in Hg accumulation in RDC312 occurred at similar times as two of the events identified in BRW100 (ca. 1972 and ca. 1983).

Controls on mercury accumulation and concentration

Mercury accumulation rate (µg/m^2/year) is the product of sedimentation rate and Hg concentration. To determine which of these variables was the dominant control, Hg accumulation rates were related to both sedimentation rate and
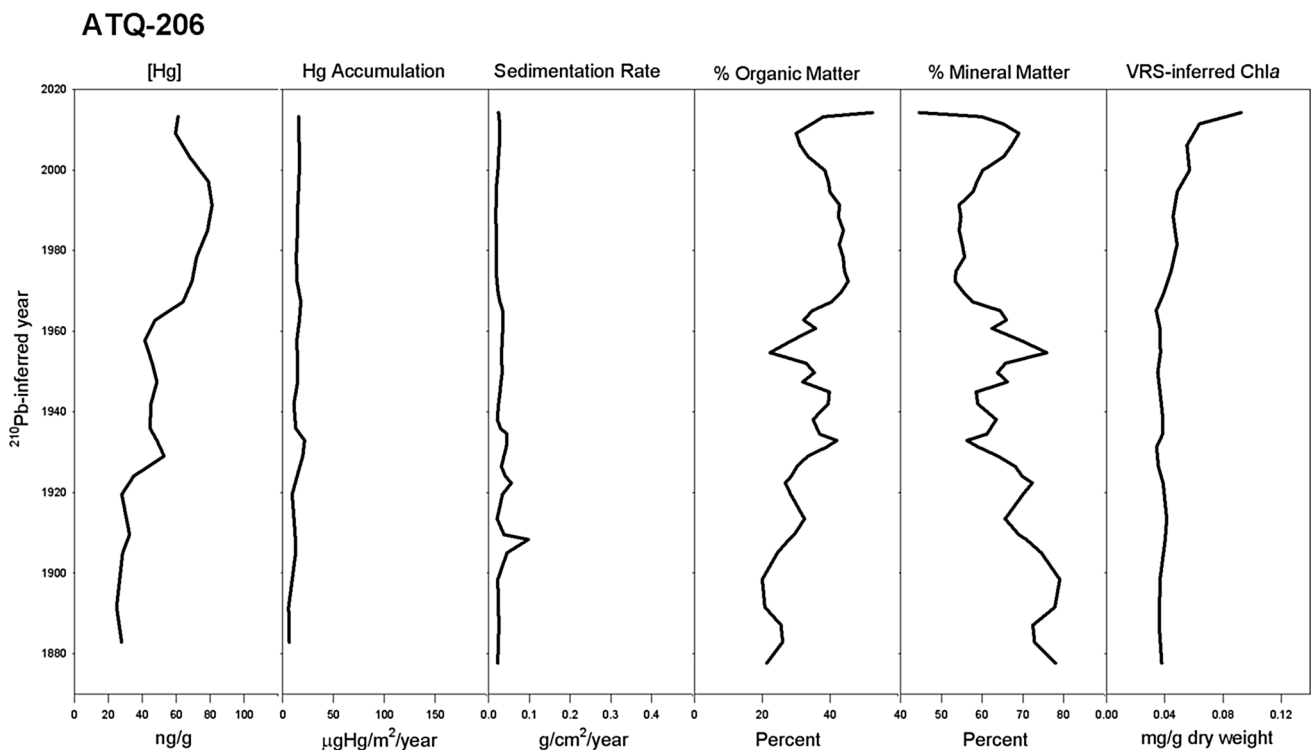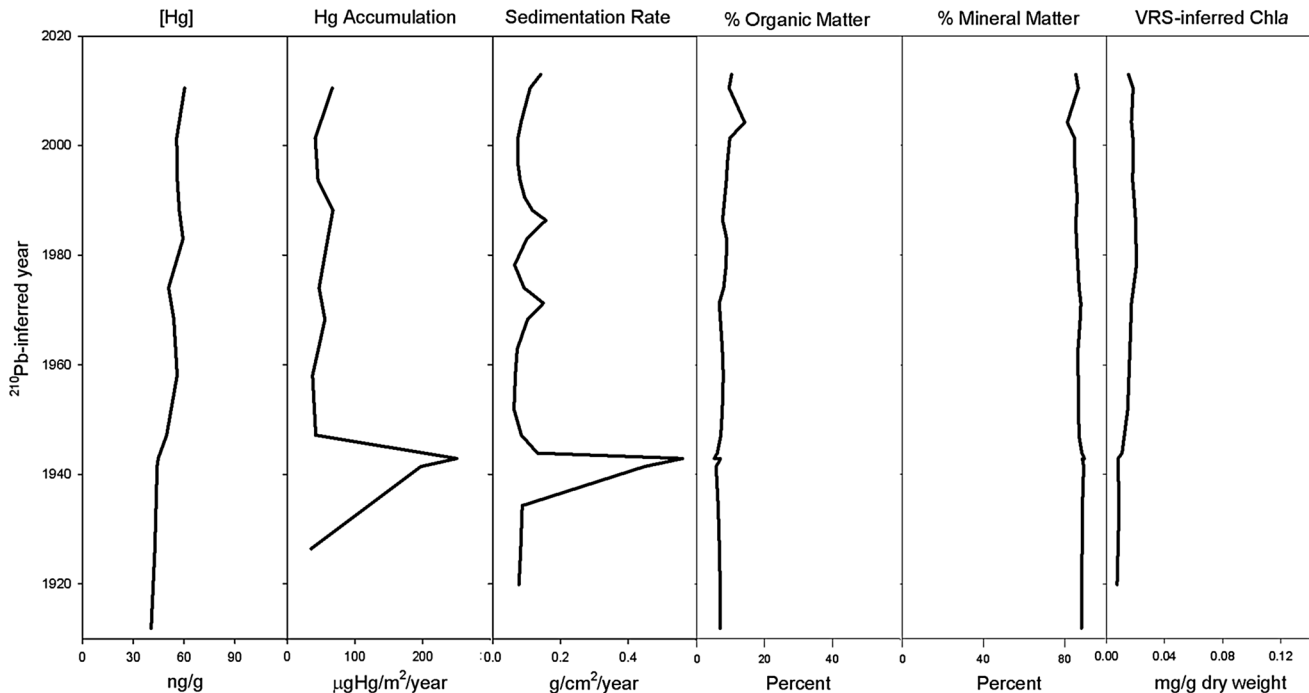

Fig. 3 Temporal profiles of sediment mercury concentration, accumulation rate, sedimentation rate, percent organic matter, percent mineral matter, and VRS-inferred chlorophyll a for lake ATQ206 on the Arctic Coastal Plain of Alaska sampled in August 2014

RDC-312

Fig. 4 Temporal profiles of sediment mercury concentration, accumulation rate, sedimentation rate, percent organic matter, percent mineral matter, and VRS-inferred chlorophyll a for lake RDC312 on the Arctic Coastal Plain of Alaska sampled in August 2014

[Hg] using linear regressions applied to data from each of the three lakes. In both BRW100 and RDC312, nearly all (97% and 99%, respectively) of the variability in Hg accumulation rate was explained by sedimentation rate (simple linear regression, $F_{1,13}=400.75$, $p < 0.001$, $r^2 = 0.97$; Fig. 2 (BRW 100); $F_{1,10}=1628$, $p < 0.001$, $r^2 = 0.99$; Fig. 4 (RDC312). In ATQ 206, Hg concentration explained more of the variability in Hg accumulation ($F_{1,21}=8.75$, $p < 0.001$, $r^2 = 0.29$; Fig. 3) than sedimentation rate ($F_{1,21}=1.47$, $p = 0.24$, $r^2 = 0.07$).

Controls on Hg concentration varied among lakes. In ATQ206, where Hg accumulation was more strongly related to [Hg] than sedimentation rate, there were significant positive relationships between [Hg] and both %OM ($r^2 = 0.70$) and Chl a ($r^2 = 0.28$) (simple linear regression, $F >_{1,20} \geq 16.52$, $p < 0.001$). These positive relationships indicate that Hg delivered to ATQ206 is primarily bound to allochthonous and/or autochthonous organic matter; while we can clearly identify the contribution of autochthonous OM-bound Hg via the relationship between [Hg] and Chl a, %OM represents both authochthonous (quantifiable) and allochthonous (not quantifiable with these data) contributions. In RDC312, where Hg accumulation was more strongly related to sedimentation rate, [Hg] concentration was also significantly and positively related to %OM ($r^2 = 0.66$) and Chl a ($r^2 = 0.87$) ($F >_{1,10} \geq 19.14$, $p \leq 0.001$). In contrast,

there were significant negative relationships between [Hg] and both %OM ($r^2 = 0.50$) and Chl a ($r^2 = 0.40$) in BRW100 ($F >_{1,13} \geq 13.18$, $p \leq 0.003$), but a significant and positive relationship between %MM and [Hg] ($r^2 = 0.47$, $F_{1,13=}13.18$, $p = 0.003$). These results indicate that Hg in BRW100 sediments is likely associated more with mineral matter than with organic matter. The negative relationships between primary production and [Hg] were likely driven by increases in Chl a and OM from ~ 1999–2014, and indeed when these years were excluded from the analysis, no significant relationship existed between [Hg] and %OM ($F_{1,10}=4.03$, $p = 0.07$, $r^2 = 0.29$). The negative relationship between [Hg] and Chl a was weaker, although still significant ($F_{1,20}=5.27$, $p = 0.03$, $r^2 = 0.21$).

To identify potential causes of episodic sedimentation events (with associated increases in Hg accumulation) in BRW100 and RDC312, historical aerial images were analyzed. It appears that there were increases in lake surface area in both lakes between 1948 and 2005; surface areas of BRW100 and RDC 312 increased by 12.7% and 5.4%, respectively, during this time period (Fig. 5; Table 1). In contrast, there was a negligible change in the surface area of ATQ206 (0.3%) during this same time period (Fig. 5; Table 1). Other notable changes in lake morphometry and catchment characteristics can be discerned from the aerial imagery series. In BRW100, an access road was constructed
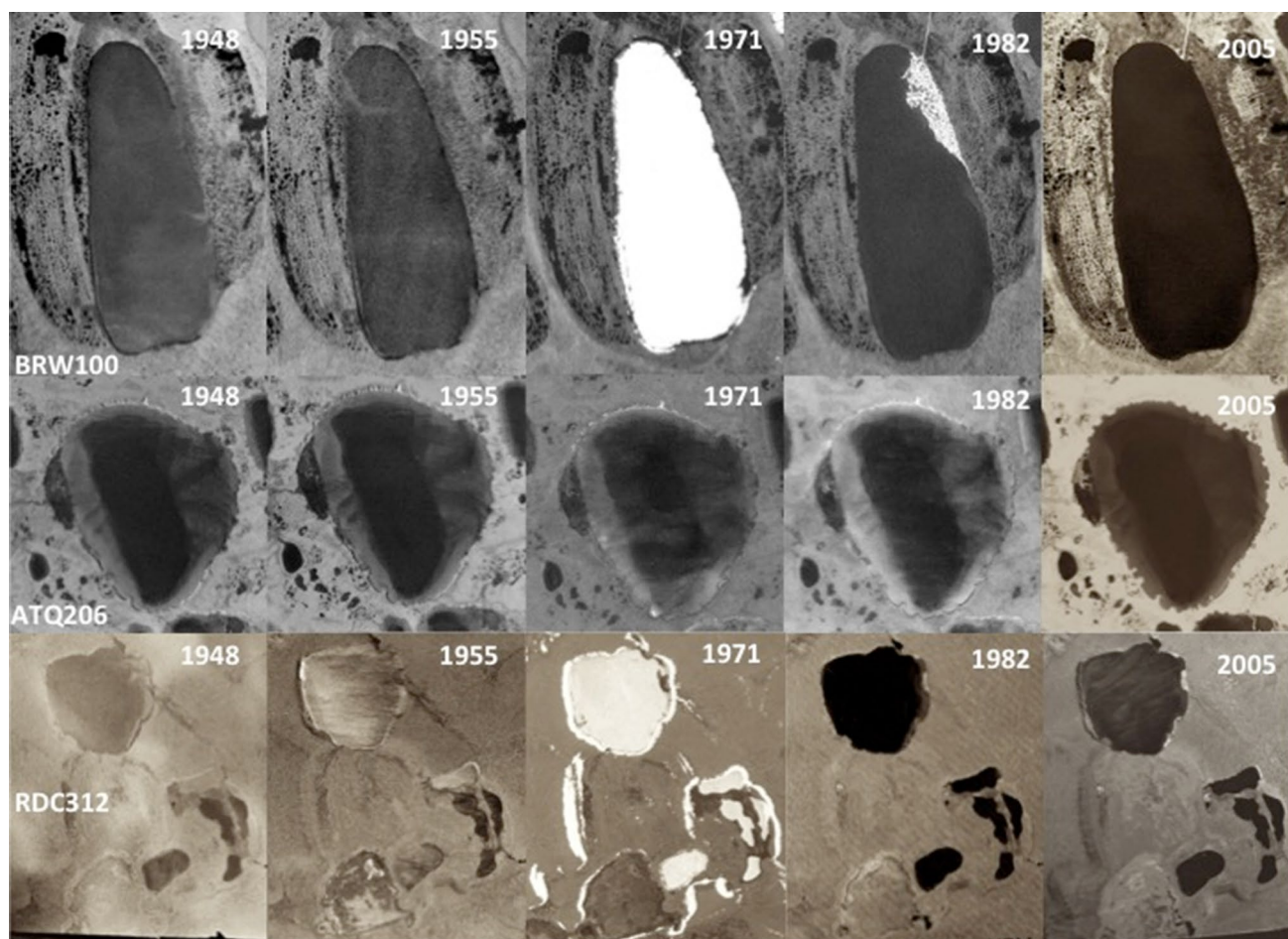
Fig. 5 Historical aerial images from 1948, 1955, 1971, 1982, and 2005 of three study lakes (BRW100, ATQ206, and RDC312) on the Arctic Coastal Plain of Alaska; the imagery is property of the United States Geological Survey (USGS 2016)

at some point between 1955 and 1973 (Fig. 5). An article outlining a funding proposal for this road narrows the window of road construction to between 1967 and 1973 (Tundra Times 1966), which is coincident with a sedimentation event that occurred in ca. 1972 (Fig. 2).

Visual interpretation of aerial imagery suggests that catchment hydrology could have contributed to the sedimentation events observed in the sediment profile for RDC3012. RDC312 has the largest relative catchment size of the three lakes (Table 1), and unique hydrological features, including an up-gradient lake complex to the south and southeast (Fig. 5). It is also evident that a shoreline collapse occurred along the eastern bank of the lake at some point (Fig. 5); however, this event predates available aerial imagery.

Comparison of mercury accumulation with other Arctic and subarctic lakes

Of the eleven additional Alaskan lakes for which data were available, the majority (8) had mean Hg accumulation rates that were most similar to that observed for ATQ206 (14.2 ± 3.60 µg/m^2/year); that is, much lower (mean Hg accumulation $= 11.2 \pm 8.8$ µg/m^2/year) and more uniform (mean temporal standard deviation $= 4.2 \pm 4.7$) than what we observed in either BRW100 (92.0 ± 36.1 µg/m^2/year) or RDC312 (78.6 ± 69.5 µg/m^2/year; Table 2). When the additional 33 Arctic lakes with available data, including the seven aforementioned Alaskan lakes, and lakes from Canada, Greenland, and Norway (Fig. 1; Table 2) were separated by landscape type (lake thermokarst, hillslope thermokarst, and non-thermokarst), significant differences were found in both mean Hg accumulation (ANOVA, $F_{2,37} = 3.66$, $p = 0.036$) and temporal variability (standard error, ANOVA, $F_{2,37} = 16.64$, $p < 0.0001$; Fig. 6). Post-hoc Tukey's tests indicated that lakes in lake thermokarst landscapes had significantly higher mean Hg accumulation than lakes in non-thermokarst landscapes ($p = 0.03$), and that Hg accumulation in lakes from lake thermokarst landscapes was significantly more temporally variable than that in hillslope thermokarst landscapes (< 0.0001) or non-thermokarst landscapes ($p < 0.0001$). The
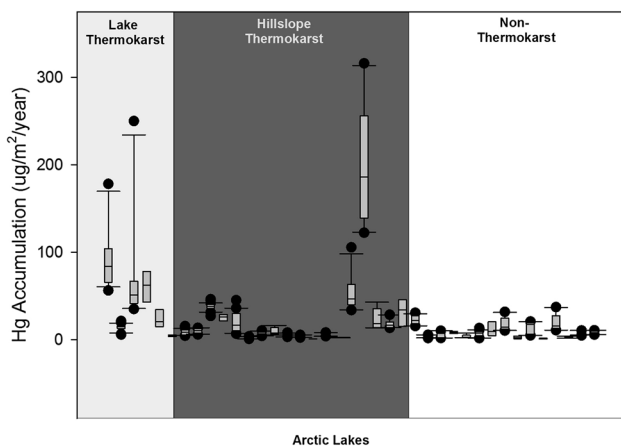
Fig. 6 Box and whisker plots for mercury accumulation rates for 37 circumarctic and 4 subarctic Alaskan lakes on different landscape types, as defined in Olefeldt et (2016). The range bars are 95% confidence intervals; boxes show the inter-quartile ranges (25–75%), the horizontal line indicates the median. The lakes in 'lake thermokarst' panel represent, in order: BRW100, ATQ206, and RDC312 (this study), and lakes 2A, and 2B (data from Deison et al. 2012). Accumulation rates are significantly higher and more variable in Lake Thermokarst lakes than Non-thermokarst lakes. Accumulation rates are focus-corrected when data were available (see Online Resource 1)

lakes that fall in the lake thermokarst landscape category include the three lakes from this study and two lakes (2A and 2B) in the Mackenzie Delta Uplands from Deison et al. (2012). Similar to BRW100 and RDC312, sedimentation rate in these two Deison et al. (2012) lakes explained almost all of the variability in Hg accumulation rate (simple linear regression $r^2 \geq 0.94$, $F >_{1,5} \geq 97.75$, $p < 0.002$).

Mercury accumulation rates increased significantly (similar to ATQ 206) in 28 of the 37 lakes for which data were acquired from the literature (Mann–Kendall, Table 2). No significant monotonic trends were observed in 7 of the lakes (Mann–Kendall, Table 2.), and a significant decrease was observed in one lake in the Mackenzie River delta (Mann–Kendall, Table 2). Including the lakes from this study, 14 of 16 (88%) non-thermokarst lakes displayed a significant increase in Hg accumulation, whereas Hg accumulation increased in 14 of 19 (74%) 'hillslope thermokarst' lakes and 2 of 5 (40%) 'lake thermokarst' lakes (see Online Resource 1).

Discussion

Controls on Hg accumulation

Of the three lakes sampled for this study, two had variable and non-directional temporal trends in Hg accumulation (BRW100 and RDC312) rates that were driven by sedimentation rate, and one lake (ATQ206) had a significant

(2.4-fold) temporal increase in Hg accumulation rate that was driven by Hg concentration. Analyses conducted on additional data collated from 37 subarctic and Arctic lakes revealed that two to three-fold increases in Hg accumulation since preindustrial times have been widely observed in lakes in the Northwest Territories (see Muir et al. 2009), Nunavut (Hermanson 1998), Norway (Drevnick et al. 2012), Greenland (Bindler et al. 2001), and Alaska (Fitzgerald et al. 2005). Observations of no directional change (see Muir et al. 2009) and/or decreases (Deison et al. 2012) in Hg accumulation were less common. Several features of BRW100 and RDC312 and their catchments may explain the relatively high and variable sedimentation rates observed, and the lack of temporal trend in Hg accumulation rate. These interpretations may be applicable to the similar trends in sedimentation and Hg accumulation rates observed for lakes 2A and 2B from Deison et al. (2012), and allow for more informed predictions and understanding of Hg accumulation rates in lakes in lake thermokarst regions (Olefeldt et al. 2016) that have similar physical characteristics.

BRW100 is a typical example of a thermokarst lake on the Arctic Coastal Plain; it is elliptical in shape, and oriented to the northwest (see Grosse et al. 2013). An access road was constructed to BRW100 between 1967 and 1973, which aligns with one of the major sedimentation events (ca 1972). Aside from possible land use change-related sediment inputs, the high and variable sedimentation rate may also reflect thermokarstic activity or surface runoff events associated with low soil hydraulic conductivity. Thermokarst lakes are subject to several shoreline erosive processes, including thermal erosion and mechanical erosion via wave action (see Grosse et al. 2013). The silty, ice-rich catchment sediments of the thermokarst lakes of the Arctic Coastal Plain make them prone to enhanced shoreline erosion (see Grosse et al. 2013), which likely contributed to lateral growth in BRW100 (12.7% since 1948), and sedimentation events not related to road construction. Sedimentation events could also reflect pulses of material delivered to BRW100 during spring snowmelt or large precipitation events; previous data indicate that the catchment soils of BRW100 are poorly drained (Jorgensen and Grunblat, 2013), and thus more prone to pulses rather than gradual and continuous sediment delivery.

While visual analysis of aerial imagery indicates that thermal shoreline erosion could have contributed to the variable and high sedimentation rate in RDC312, as it too appears to have expanded (to a lesser extent, 5.4% since 1948), it is likely that erosive processes related to terrestrial catchment hydrology (i.e., relative catchment size and presence of up-gradient lake complex) had a greater influence on sedimentation rate and thus Hg accumulation. RDC312 is not a typical thermokarst lake; although it is in a zone of continuous permafrost and in a lake thermokarst region, lake morphology and catchment composition are distinctly different from

BRW100. For example, BRW100 is surrounded by polygonal ground indicative of degrading ground ice, which is absent from the area surrounding RDC312. RDC312 is also at a higher elevation than low-relief BRW100 (as it borders Brooks Range), and has a smaller area, but larger relative catchment size. Its proximity to Brooks Range exposes it to higher storm intensities than are typical near the coast (Miller, 1963). Finally, RDC312 is located in the Arctic silty lowland, where soils are silty with a thick organic-rich surface layer. Previous data indicate that these soils likely have an even lower hydraulic conductivity than the catchment soils of BRW100 (Jorgensen and Grunblat, 2013). Large relative catchment size (compared to BRW100), and low hydraulic conductivity could facilitate overland flow and pulses of sediment (and Hg) from surface erosion. Since two of the major sedimentation events in each of BRW100 and RDC312 occurred around the same time (early 1970s and mid 1980s) it is possible that they were triggered by regional weather events (e.g., high precipitation, abnormally warm or windy year), although the 1972 BRW100 event was almost certainly driven by the road construction. BRW100 and RDC312 had variable and high sedimentation and Hg accumulation rates, and we suggest that this is largely due to a combination of thermokarst activity and runoff over catchment soils with low hydraulic conductivity. We suspect that similar factors explain the variable and high sedimentation and Hg accumulation rates in lakes 2A and 2B from Deison et al. (2012).

Compared to the other four lakes located within a lake thermokarst region, ATQ206 had relatively low and consistent Hg accumulation rates that were more similar to those observed further south in Arctic Alaska. There was a significant increase over time in Hg accumulation in ATQ206, and the magnitude of this increase was similar to what was observed in the five Alaskan lakes near the Toolik Field Station originally investigated by Fitzgerald et al. (2005). These five lakes collectively showed a ~ 2.5-fold increase in Hg accumulation rates since preindustrial times (before ca.1850), which the authors attributed to a combination of increases in atmospheric deposition and enhanced erosion of soils (Fitzgerald et al. 2005). While the sediment core from ATQ206 did not quite extend to pre-industrial times (pre-1850), a similar 2.4-fold increase was observed in Hg accumulation between 1883 and 2013. Although the lakes studied by Fitzgerald et al. (2005) are much smaller in surface area than ATQ206, the Fitzgerald et al. (2005) lakes have several physical attributes that are similar to ATQ206 (e.g. relatively small catchment to surface area ratio, coarse catchment sediments) and that could explain why sedimentation and Hg accumulation rates in these lakes were dissimilar to those observed in BRW100 and RDC312.

Relatively high hydraulic conductivity in ATQ206 and in the Fitzgerald et al. (2005) lakes may partially explain the relatively low and invariable sedimentation rates and the relatively low Hg accumulation rates in these lakes. The Fitzgerald et al. (2005) lakes and ATQ206 have catchment soils with a greater fraction of sands (Fitzgerald et al. 2005; Jorgensen and Grunblat, 2013). These coarse catchment sediments likely have higher hydraulic conductivity; hydraulic conductivity tests on soils near ATQ206 in the Arctic sandy lowland, and on soils near RDC312 in the Arctic silty lowland, indicated that soils near ATQ206 were twice as conductive as those near RDC312 (J. Koch, unpublished data). While conductivity tests were not performed near BRW100, catchment conductivity is likely low (relative to ATQ206), since it is located in the Arctic peaty-sandy lowland, where soils in swales are poorly drained (Jorgenson and Grunblatt 2013). We suggest that the relatively low sedimentation and Hg accumulation rates in ATQ206 and the Fitzgerald lakes (when compared to BRW100 and RDC312) can be explained by a combination of high hydraulic conductivity, small relative catchment sizes, and an absence of catchment land-use disturbance and appreciable thermokarst activity (e.g., thermal erosion/lateral expansion, or slumping).

Mercury accumulation rates were more strongly related to Hg concentration than sedimentation rates in ATQ206, and Hg concentration was positively related with both %OM and VRS-inferred Chl *a* in both ATQ206 and RDC312. In BRW100, Hg concentration was negatively related to both %OM and VRS-inferred Chl *a*. Positive relationships between Hg concentration and indicators of lake primary production (%OM and VRS-inferred Chl *a*) in ATQ206 and RDC312 can be explained by the affinity of the oxidized Hg species, Hg(II), for reduced complexes in organic matter (e.g., thiols; see Ravichandran 2003). This complexation can occur in (but is not restricted to) the lake or in the catchment, and as such the transfer of OM from the terrestrial catchment can be an important source of Hg. Since we did not quantify the proportion of OM originating from the terrestrial catchment (allochthony) versus the lake (autochthony) it is difficult to disentangle the positive relationships between Hg concentration and %OM; however it is likely that both allochthonous and authochonous sources contributed to the OM in each of the lakes. Many researchers have attributed post-industrial increases in Hg accumulation to a form of autochthonous complexation termed "algal scavenging" (Outridge et al. 2007; Stern et al. 2009). Algal scavenging could explain the positive relationship between Hg concentration and Chl *a* observed in ATQ206 and RDC312. The negative relationship between Hg concentration and primary production in BRW100 is less straightforward. Unlike ATQ206, RDC312, and many temperate lakes, the Hg in this lake is not primarily associated with organic, but rather minerogenic matter, as evidenced by the significant positive relationship with %MM. Although Hg can be deposited directly onto lakes, it is clear from the strong relationship between

sedimentation rate and Hg accumulation that catchment contributions have historically been important in Hg delivery to BRW100. The negative relationship between %OM and Hg concentration was driven by samples that represent the time period 1999–2014, when an increase in autochthonous primary production (indicated by Chl *a*) was observed. Since Hg is more closely associated with minerogenic matter in this lake, it is possible that the increase in number of algal cells resulting from greater primary production decreased the Hg concentration in each algal cell (and consequently the sediment), via a similar mechanism to bloom dilution (Pickhardt et al. 2002). This inference is supported by the fact that when the years 1999–2014 (when a noticeable increase in Chl *a* was observed) are excluded from the analysis, there is no relationship between [Hg] and %OM.

The future of Hg accumulation in thermokarst lakes

Results from this study allow for some predictions about future trends in Hg concentration and accumulation in thermokarst lakes. As temperatures continue to rise, growing seasons will lengthen, and there will likely be a continued increase in autochthonous primary production (i.e., more algal cells) in Arctic lakes (Prowse et al. 2006). Additionally, rising temperatures are expected to result in increases in thermokarstic activity (e.g., thermal erosion, thaw slumping; see Grosse et al. 2013), and enhanced runoff (Barnett et al. 2005), which could increase the amount of terrestrial organic matter entering lakes from catchment sources. As the data from this study indicate, each of these climate-affected processes could have disparate effects on sediment Hg concentration depending on the fraction (i.e., organic matter or minerogenic matter) with which the Hg in a given lake is most closely associated, and the composition/conductivity of catchment soils. Our results suggest that an increase in primary production could lead to an increase in sediment Hg concentration in both ATQ206 and RDC312 due to complexation with organic matter (i.e., algal scavenging), and a decrease in sediment Hg concentration in BRW100 due to dilution of minerogenic sediments. There is also potential for an increase in sediment Hg concentration in RDC312 due to either increased runoff or enhanced thermokarstic activity, as its catchment has a thick organic surface layer. Since Hg concentration was the dominant driver of Hg accumulation in ATQ206, if sedimentation rates in this lake remain low and steady, an increase in Hg accumulation could be expected with increased primary productivity. Conversely, if sedimentation rates in BRW100 and RDC312 remain high and variable, an increase in primary production (and concomitant increases and decreases in Hg concentration in RDC312 and BRW100, respectively) would likely not have a notable impact on Hg accumulation in these lakes, since sedimentation rate is the dominant driver of Hg accumulation.

Predicted temperature-driven increases in primary production and thermokarstic activity in Arctic regions are well documented; however, these processes are not always collinear. Longer ice-free seasons should lead to an increase in phytoplankton production, as seen in BRW100 and ATQ206 in this study (e.g., Prowse et al. 2002); however, thermokarstic events such as retrogressive thaw slumps (prominent in hillslope thermokarst landcapes) have been found to decrease phytoplankton production (Thienpont et al. 2013). Although the temporal scale and resolution of aerial photograph coverage precluded the direct assessment of thaw slump activity in this study, it is important to consider the potential mechanisms thaw slumping could drive. A thaw slump results in a massive amount of permafrost soil entering a lake. Permafrost soils have comparatively higher ionic concentration than the overlying active layer due to persistent leaching, so concentrated solutes enter the system with the sediment (Kokelj and Lewkowicz 1999; Kokelj and Burn 2003). Base cations facilitate the absorption and flocculation of humic substances (coloured dissolved organic matter), and although the inundation of ion-rich minerogenic soils from a thaw slump may temporarily limit light, it can lead to greater water clarity in the long term (Thompson et al. 2008). This increased clarity can lead to increased macrophyte growth, and potentially a shift away from phytoplankton dominance (Thompson et al. 2008), which could decrease sediment [Hg] by reducing the capacity for "algal-scavenging". Of the three study lakes, RDC312 is the only lake that is currently macrophyte-dominated; however, it is unclear how long it has been in this state. Additionally, thaw slumping itself can lead to a dilution of Hg in surface sediments (Deison et al. 2012). Thus, effects of rising temperatures on Hg accumulation and concentration in thermokarstic lake sediments will depend on catchment size and catchment sediment composition, as well as a variety of variables that control primary productivity, and frequency and magnitude of thermokarstic events.

Future Hg accumulation rates in the study lakes could also reflect changes in atmospheric deposition (Fitzgerald et al. 2005). Although the lakes studied here have not historically displayed a distinct atmospheric Hg signal (increase to peak Hg concentrations in 1970s followed by recent decrease (e.g., Engstrom and Swain 1997)), it is possible that this could change. Legislation has led to a decrease in Hg emissions by the power sector in North America since the 1980s (Slemr et al. 2003); however, since this legislation is not globally applicable and Arctic Alaska receives considerable Hg inputs from Asia and Russia (see AMAP 2011), future emissions are unpredictable. If emissions were to continue to decline, it could have an impact on Hg concentration and accumulation in the Arctic Coastal Plain lakes. Changes in emissions would likely be detected first in lakes with small relative catchment sizes, like ATQ206 and BRW100, before

lakes with large relative catchment sizes, like RDC312, due to the important and longer-term influence of Hg (both anthropogenic and natural) stored in catchment soils (see Grigal 2002; Fitzgerald et al. 2005; Harris et al. 2007). Further research is required to effectively predict the timeframe and magnitude of the impact of reduced atmospheric emissions on Hg in lake sediments.

Thermokarst landscapes cover more than 20% of the northern permafrost region (Olefeldt et al. 2016), and available data from this study and previously published work suggest that the highest and most variable Hg accumulation rates occur in lakes in thermokarst regions. We suggest that low hydraulic conductivity and thermokarstic processes (e.g., thermal erosion, retrogressive thaw slumps) lead to high and variable Hg accumulation rates. Available data cover only a fraction of the global thermokarst landscape (i.e., lake thermokarst and hillslope thermokarst); however, the vast majority of this landscape is located in Arctic Russia, where presumably lakes with variable and high Hg accumulation rates also exist.

Conclusions

Results of this study demonstrate that lakes on the Arctic Coastal Plain of Alaska have variable Hg accumulation histories with different underlying controls. Sedimentation rate drove Hg accumulation in the lakes where it was found to be high and variable, and high and variable sediment and Hg accumulation rates were more prevalent in lakes on thermokarst landscapes than on non-thermokarst landscapes. It can be inferred that Hg accumulation in other lakes with similar characteristics (i.e., ice rich catchment sediments, large relative catchment size, and low hydraulic conductivity) on 'lake thermokarst' or 'hillslope thermokarst' landscapes could also be driven by sedimentation rate. Conversely, Hg accumulation rates in lakes with small relative catchment sizes and conductive catchment soils could be driven more by factors that control Hg concentration, such as primary production and organic matter inputs. It is imperative that variability in landscape setting and lake physical characteristics, such as relative catchment size, catchment soil composition (grain size, ice content), and hydraulic conductivity, are reflected in predictions of future Hg accumulation in Arctic lakes.

References

Allen-Gil SM, Gubala C, Landers D, Lasorsa B, Crecelius E, Curtis L (1997) Heavy metal accumulation in sediment and freshwater fish in US Arctic lakes. Environ Toxicol Chem 16(4):733–741

Appleby PG, Oldfield F (1978) The calculation of lead-210 dates assuming a constant rate of supply of unsupported 210 Pb to the sediment. Catena 5(1):1–8

Arctic Monitoring and Assessment Programme (2011) Mercury in the Arctic. Arctic Monitoring and Assessment Programme (AMAP), Oslo, Norway. xiv. p. 191

Arctic Monitoring and Assessment Programme (AMAP) and United Nations Environment Programme (UNEP) (2013) Technical Background Report for the Global Mercury Assessment. UNEP Chemicals Branch: Geneva

Atwell L, Hobson K, Welch H (1998) Biomagnification and bioaccumulation of mercury in an arctic marine food web: insights from stable nitrogen isotope analysis. Can J Fish Aquat Sci 55(5):1114–1121

Barnett T, Adam J, Lettenmaier D (2005) Potential impacts of a warming climate on water availability in snow-dominated regions. Nature 438(7066):3 03

Biester H, Bindler R, Martinez-Cortizas A, Engstrom D (2007) Modeling the past atmospheric deposition of mercury using natural archives. Environ Sci Technol 41(14):4851–4860

Bindler R, Olofsson C, Renberg I, Frech W (2001) Temporal trends in mercury accumulation in lake sediments in Sweden. Water Air Soil Pollut Focus 1(3–4):343–355

Bookman R, Driscoll C, Engstrom D, Effler S (2008) Local to regional emission sources affecting mercury fluxes to New York lakes. Atmos Environ 42(24):6088–6097

Bravo AG, Bouchet S, Tolu J, Bjorn E, Mateos-Rivera A, Bertilsson S (2017) Molecular composition of organic matter controls methylmercury formation in boreal lakes. Nat Commun 8(14255). https://doi.org/10.1038/ncomms14255

Dean WE (1974) Determination of carbonate and organic matter in calcareous sediments and sedimentary rocks by loss on ignition: comparison with other methods. J Sediment Res 44(1):242–248

Deison R, Smol J, Kokelj S, Pisaric M, Kimpe L, Poulain A et al (2012) Spatial and temporal assessment of mercury and organic matter in thermokarst affected lakes of the Mackenzie Delta Uplands, NT, Canada. Environ Sci Technol 46(16):8748–8755

Drevnick PE, Yang H, Lamborg C, Rose N (2012) Net atmospheric mercury deposition to Svalbard: Estimates from lacustrine sediments. Atmos Environ 59:509–513

Drevnick PE, Cooke C, Barraza D, Blais J, Coale K, Cumming B et al (2016) Spatiotemporal patterns of mercury accumulation in lake sediments of western North America. Sci Total Environ 568:1157–1170

Driscoll CT, Mason R, Chan H, Jacob D, Pirrone N (2013) Mercury as a global pollutant: sources, pathways, and effects. Environ Sci Technol 47(10):4967–4983

Engstrom DR, Swain E (1997) Recent declines in atmospheric mercury deposition in the upper Midwest. Environ Sci Technol 31(4):960–967

Engstrom DR, Balogh S, Swain E (2007) History of mercury inputs to Minnesota lakes: influences of watershed disturbance and localized atmospheric deposition. Limnol Oceanogr 52(6):2467–2483

Environmental Systems Research Institute (ESRI) (2016) ArcGIS Desktop: release 10. Redlands, CA: Environmental Systems (software)

Fitzgerald WF, Engstrom D, Lamborg C, Tseng C, Balcom PH, Hammerschmidt C (2005) Modern and historic atmospheric mercury fluxes in northern Alaska: global sources and Arctic depletion. Environ Sci Technol 39(2):557–568

Grigal DF (2002) Inputs and outputs of mercury from terrestrial watersheds: a review. Environ Rev 10(1):1–39

Grosse G, Jones B, Arp C (2013) Thermokarst lakes, drainage, and drained Basins. In: Shroder J (ed) Treatise on geomorphology, vol 8, glacial and periglacial geomorphology. Academic Press, San Diego, pp 325–353

Harris RC, Rudd J, Amyot M, Babiarz C, Beaty K, Blanchfield P et al (2007) Whole-ecosystem study shows rapid fish-mercury response to changes in mercury deposition. Proc Natl Acad Sci USA 104(42):16586–16591

Hermanson MH (1998) Anthropogenic mercury deposition to Arctic lake sediments. Water Air Soil Pollut 101(1–4):309–321

Jorgenson MT, Grunblatt J (2013). Landscape-level ecological mapping of northern Alaska and field site photography. Report prepared for the Arctic Landscap Conservation Cooperative. http://arcticlcc.org/assets/products/ALCC2011-06/reports/NorthernAK_Landscape_ Mappping_Field_Photos_Final_RPT pdf

Jorgenson MT, Shur Y (2007) Evolution of lakes and basins in northern Alaska and discussion of the thaw lake cycle. J Geophys Res 112: F02S17

Kamman NC, Engstrom D (2002) Historical and present fluxes of mercury to Vermont and New Hampshire lakes inferred from 210 Pb dated sediment cores. Atmos Environ 36(10):1599–1609

Kidd KA, Hesslein RH, Fudge R, Hallard K (1995) The influence of trophic level as measured by δ 15N on mercury concentrations in freshwater organisms. Wat Air Soil Pollut 80:1011–1015

Kirk JL, Muir D, Antoniades D, Douglas M, Evans M, Jackson T et al (2011) Climate change and mercury accumulation in Canadian high and subarctic lakes. Environ Sci Technol 45:964–970

Kokelj SV, Burn C (2003) Ground ice and soluble cations in near-surface permafrost, Inuvik, Northwest Territories, Canada. Permafrost Periglac 14(3):275–289

Kokelj SV, Lewkowicz A (1999) Salinization of permafrost terrain due to natural geomorphic disturbance, Fosheim Peninsula, Ellesmere Island. Arctic 52:372–385

Landers DH, Gubala C, Verta M, Lucotte M, Johansson K, Vlasova T, Lockhart W (1998) Using lake sediment mercury flux ratios to evaluate the regional and continental dimensions of mercury deposition in arctic and boreal ecosystems. Atmos Environ 32(5):919–928

Lockhart WL, Stern G, Wagemann R, Hunt R, Metner D, DeLaronde J et al (2005) Concentrations of mercury in tissues of beluga whales (Delphinapterus leucas) from several communities in the Canadian Arctic from 1981 to 2002. Sci Total Environ 351:391–412

Lorey P, Driscoll C (1999) Historical trends of mercury deposition in Adirondack lakes. Environ Sci Technol 33(5):718–722

McLeod AI (2011) Kendall: Kendall rank correlation and Mann-Kendall trend test. R package version 2.2. https://CRAN.R-project.org/package=Kendall

Michelutti N, Blais J, Cumming B, Paterson A, Rühland K, Wolfe A, Smol J (2010) Do spectrally inferred determinations of chlorophyll a reflect trends in lake trophic status? J Paleolimnol 43(2):205–217

Muir DCG, Wang X, Yang F, Nguyen N, Jackson T, Evans MS et al (2009) Spatial trends and historical deposition of mercury in eastern and northern Canada inferred from lake sediment cores. Environ Sci Technol 43(13):4802–4809

Olefeldt D, Goswami S, Grosse G, Hayes D, Hugelius G, Kuhry P, McGuire A, Romanovsky V, Sannel A, Schuur E, Turetsky M (2016) Circumpolar distribution and carbon storage of thermokarst landscapes. Nat Commun DOI. https://doi.org/10.1038/ncomms13043

Oswald CJ, Heyes A, Branfireun B (2014) Fate and Transport of Ambient Mercury and Applied Mercury Isotope in Terrestrial Upland Soils: Insights from the METAALICUS Watershed. Environ Sci Technol 48(2):1023–1031

Outridge PM, Sanei H, Stern G, Hamilton P, Goodarzi F (2007) Evidence for control of mercury accumulation rates in Canadian High Arctic lake sediments by variations of aquatic primary productivity. Environ Sci Technol 41(15):5259–5265

Pickhardt PC, Folt C, Chen C, Klaue B, Blum J (2002) Algal blooms reduce the uptake of toxic methylmercury in freshwater food webs. Proc Natl Acad Sci USA 99(7):4419–4423

Prowse TD, Wrona F, Reist J, Gibson J, Hobbie J, Lévesque L, Vincent W (2006) Climate change effects on hydroecology of Arctic freshwater ecosystems. Ambio 35(7):347–358

R Core Team (2017). R: A language and environment for statistical computing. R Foundation for Statistical Computing, Vienna http://www.R-project.org/

Ravichandran M (2004) Interactions between mercury and dissolved organic matter—a review. Chemosphere 55(3):319–331

Rohatgi A (2016). Web plot digitizer. Austin, TX (software)

Slemr F, Brunke E, Ebinghaus R, Temme C, Munthe J, Wängberg I et al (2003) Worldwide trend of atmospheric mercury since 1977. Geophys Res Lett 30:1516. doi:https://doi.org/10.1029/2003GL016954

Stern GA, Sanei H, Roach P, Delaronde J, Outridge P (2009) Historical interrelated variations of mercury and aquatic organic matter in lake sediment cores from a subarctic lake in Yukon, Canada: further evidence toward the algal-mercury scavenging hypothesis. Environ Sci Technol 43(20):7684–7690

Thienpont JR, Rühland K, Pisaric M, Kokelj S, Kimpe L, Blais J, Smol J (2013) Biological responses to permafrost thaw slumping in Canadian Arctic lakes. Freshwater Biol 58(2):337–353

Thompson MS, Kokelj S, Prowse T, Wrona F (2008) The impact of sediments derived from thawing permafrost on tundra lake water chemistry: An experimental approach. In Proc 9th Int Conf on Permafrost. (University of Alaska, Fairbanks) 2:1763–1768

Tundra Times (1966) Sen to ask for $350 000 for road. Tundra Times, Barrow, AK

U.S. Environmental Protection Agency (EPA) (2007) Method 7473 e Mercury in Solids and Solutions by Thermal Decomposition, Amalgamation, and Atomic Absorption Spectrophotometry, Revision 0. http://www.epa.gov/osw/hazard/testmethods/ sw846/pdfs/7473.pdf

U.S. Geological Survey (USGS) (2016) Earth Explorer. Earth Resources Observation and Science (EROS) Center, Sioux Falls, SD (software)

Wolfe AP, Vinebrooke R, Michelutti N, Rivard B, Das B (2006) Experimental calibration of lake-sediment spectral reflectance to chlorophyll a concentrations: methodology and paleolimnological validation. J Paleolimnol 36(1):91–100

Yang H, Rose N (2003) Distribution of mercury in six lake sediment cores across the UK. Sci Total Environ 304(1):391–404